Vaccine and Wild-Type Strains of Yellow Fever Virus Engage Distinct Entry Mechanisms and Differentially Stimulate Antiviral Immune Responses

Maria Dolores Fernandez-Garcia, Laurent Meertens, Maxime Chazal, Mohamed Lamine Hafirassou, Ophélie Dejarnac, Alessia Zamborlini, Philippe Desprès, Nathalie Sauvonnet, Fernando Arenzana-Seisdedos, Nolwenn Jouvenet, et al.

AMERICAN SOCIETY FOR MICROBIOLOGY | mBio®

RESEARCH ARTICLE

Vaccine and Wild-Type Strains of Yellow Fever Virus Engage Distinct Entry Mechanisms and Differentially Stimulate Antiviral Immune Responses

Maria Dolores Fernandez-Garcia,[a,b,c]* Laurent Meertens,[a,b,c] Maxime Chazal,[d] Mohamed Lamine Hafirassou,[a,b,c] Ophélie Dejarnac,[a,b,c] Alessia Zamborlini,[a,b,c,e] Philippe Despres,[f] Nathalie Sauvonnet,[g] Fernando Arenzana-Seisdedos,[h] Nolwenn Jouvenet,[d] Ali Amara[a,b,c]

INSERM U944-CNRS 7212, Laboratoire de Pathologie et Virologie Moleculaire, Paris, France[a]; Institut Universitaire d'Hématologie, Paris, France[b]; Université Paris Diderot, Sorbonne Paris Cité, Paris, France[c]; UMR CNRS 3569, Viral Genomics and Vaccination Unit, Pasteur Institute, Paris, France[d]; Laboratoire PVM, Conservatoire des Arts et Metiers, Paris, France[e]; Université de La Réunion, UM 134 PIMIT, INSERM U1187, CNRS UMR9192, IRD UMR 249, plate-forme technologique CYROI, 97490 Sainte-Clotilde, France[f]; Molecular Microbial Pathogenesis, INSERM U1202, Institut Pasteur, Paris, France[g]; Unité Pathogénie Virale, INSERM U819, Institut Pasteur, Paris, France[h]

* Present address: Maria Dolores Fernandez-Garcia, Institut Pasteur, Dakar, Senegal.

M.D.F.-G. and L.M. contributed equally to this article.

ABSTRACT **The live attenuated yellow fever virus (YFV) vaccine 17D stands as a "gold standard" for a successful vaccine. 17D was developed empirically by passaging the wild-type Asibi strain in mouse and chicken embryo tissues. Despite its immense success, the molecular determinants for virulence attenuation and immunogenicity of the 17D vaccine are poorly understood. 17D evolved several mutations in its genome, most of which lie within the envelope (E) protein. Given the major role played by the YFV E protein during virus entry, it has been hypothesized that the residues that diverge between the Asibi and 17D E proteins may be key determinants of attenuation. In this study, we define the process of YFV entry into target cells and investigate its implication in the activation of the antiviral cytokine response. We found that Asibi infects host cells exclusively via the classical clathrin-mediated endocytosis, while 17D exploits a clathrin-independent pathway for infectious entry. We demonstrate that the mutations in the 17D E protein acquired during the attenuation process are sufficient to explain the differential entry of Asibi versus 17D. Interestingly, we show that 17D binds to and infects host cells more efficiently than Asibi, which culminates in increased delivery of viral RNA into the cytosol and robust activation of the cytokine-mediated antiviral response. Overall, our study reveals that 17D vaccine and Asibi enter target cells through distinct mechanisms and highlights a link between 17D attenuation, virus entry, and immune activation.**

IMPORTANCE **The yellow fever virus (YFV) vaccine 17D is one of the safest and most effective live virus vaccines ever developed. The molecular determinants for virulence attenuation and immunogenicity of 17D are poorly understood. 17D was generated by serially passaging the virulent Asibi strain in vertebrate tissues. Here we examined the entry mechanisms engaged by YFV Asibi and the 17D vaccine. We found the two viruses use different entry pathways. We show that the mutations differentiating the Asibi envelope (E) protein from the 17D E protein, which arose during attenuation, are key determinants for the use of these distinct entry routes. Finally, we demonstrate that 17D binds and enters host cells more efficiently than Asibi. This results in a higher uptake of viral RNA into the cytoplasm and consequently a greater cytokine-mediated antiviral response. Overall, our data provide new insights into the biology of YFV infection and the mechanisms of viral attenuation.**

Received 18 December 2015 **Accepted** 12 January 2016 **Published** 9 February 2016

Citation Fernandez-Garcia MD, Meertens L, Chazal M, Hafirassou ML, Dejarnac O, Zamborlini A, Despres P, Sauvonnet N, Arenzana-Seisdedos F, Jouvenet N, Amara A. 2016. Vaccine and wild-type strains of yellow fever virus engage distinct entry mechanisms and differentially stimulate antiviral immune responses. mBio 7(1):e01956-15. doi:10.1128/mBio.01956-15.

Editor Terence S. Dermody, Vanderbilt University School of Medicine

Address correspondence to Nolwenn Jouvenet, jouvenet@pasteur.fr, or Ali Amara, ali.amara@inserm.fr.

Yellow fever virus (YFV) is the prototype member of the genus *Flavivirus*, a group of arthropod-borne human pathogens that includes the four dengue virus (DV) serotypes and West Nile virus (WNV) (1). YFV is a small, enveloped virus harboring a single positive-strand RNA genome of 11 kb. The genome encodes a polyprotein that is cleaved co- and posttranslationally into three structural proteins (capsid [C], membrane precursor [prM], and envelope [E]), and seven nonstructural proteins (NS1, NS2A, NS2B, NS3, NS4A, NS4B, and NS5). The C, prM, and E proteins are incorporated into virions, while NS proteins are found only in infected cells (2). NS proteins coordinate RNA replication and viral assembly and modulate innate immune responses (2).

YFV infection in humans causes broad clinical symptoms, ranging from unapparent infection to severe forms with hemorrhage and acute hepatic and renal failures (3). In humans, YFV primarily targets the liver, but other tissues, such as heart, kidneys,

and lungs, are also sites of replication (3). The live attenuated YFV vaccine 17D is one of the most effective vaccines ever generated. It has been used safely and effectively in more than 600 million individuals over the past 70 years (4). 17D replication peaks at around 5 to 7 days postvaccination and subsequently dissipates. Despite such efficacy, the molecular determinants for virulence attenuation and immunogenicity of 17D are poorly understood (5, 6). 17D was developed by passaging the wild-type (WT) and virulent strain Asibi (isolated from the blood of a human patient in 1927) in rhesus macaques and mouse and chicken embryo tissues (7). The adaptation of 17D to these tissues resulted in loss of neurotropism and viscerotropism, a property that accounts for the major disease manifestations of yellow fever in primates (5, 6). Comparison of the WT Asibi and attenuated 17D vaccines revealed that they differ by 32 amino acid substitutions and 4 nucleotides in their 3′ untranscribed region (UTR) (8). Of particular interest is the observation that the E protein is the most heavily mutated region, with 12 amino acid differences (8). As for other flaviviruses, the E protein of YFV covers most of the surface of the virion in the form of 90 dimers and dictates cell tropism, host range, and pathogenesis (1, 6). During YFV infection, the E protein binds to a still uncharacterized entry receptor(s) that targets virus particles to endosomes. Acidification triggers major conformational changes in the E protein that induce fusion of the viral and host cell membranes, resulting in the release of the viral capsid and genomic RNA into the cytoplasm. Since the E protein is a key determinant in YFV entry, the significant variation between Asibi and 17D in this region has been hypothesized to play a major role in attenuation and immunogenicity (8–11). Such differences are thought to alter the conformation of the E protein, receptor usage, and/or the process of virus internalization.

Given the effectiveness of 17D, several studies have investigated the immune response in healthy subjects receiving the vaccine. Indeed, 17D infection leads to an integrated immune response that includes several effector arms of the innate immune response (e.g., complement, inflammasome, and robust interferon [IFN] responses), as well as rapid activation of T cell immunity and production of neutralizing antibodies (6, 12–14). These studies, however, did not address differences between the vaccine strain and the parental virus. In fact, in the absence of information about how Asibi activates immune responses, it is difficult to determine true correlates of vaccine immunity.

In this study, we have defined the mechanism by which the YFV Asibi and 17D strains enter target cells and studied its implication in the activation of the antiviral cytokine response.

RESULTS

The 17D vaccine binds to and infects human cells more efficiently than the parental strain Asibi. We first compared the ability of the attenuated and parental YFV strains to infect a panel of human cells. HeLa and HEK293T cells, skin fibroblasts (HFFs), and immature dendritic cells (iDCs) were infected with 17D or Asibi at two different multiplicities of infection (MOI). Infection was scored 24 h later by flow cytometry using anti-E protein antibodies (Ab) or by measuring the viral RNA amplification at 8 h postinfection (Fig. 1A and B). All of the cells tested were more susceptible to the vaccine 17D than the parental strain Asibi (Fig. 1A and B). We obtained similar results with the hepatocyte cell lines Huh7 and HepG2 (see Fig. S1 in the supplemental material), as previously shown (15). Because most of the amino acid differences between 17D and Asibi are located in the E protein that mediates virus binding, we investigated whether enhanced 17D replication is linked to increased virus binding and viral RNA uptake. HeLa cells were incubated with Asibi or 17D for 1 h at 4°C. After being washed to eliminate unbound particles, cells were lysed immediately or after an additional incubation for 2 h at 37°C, and cell-associated viral RNAs were quantified by quantitative PCR (qPCR). We found that at both time points, a greater amount of viral RNA was associated with 17D-infected cells (Fig. 1C and D). These data indicate that the difference in the infection profiles between 17D and Asibi strains occurs as the result of increased binding to the cell surface and subsequent enhanced virus uptake and RNA delivery in the cytosol for the vaccine strain.

17D and Asibi use distinct endocytic routes for infectious entry. Clathrin-mediated endocytosis (CME) is the pH-dependent internalization route used by the majority of flaviviruses for infectious entry (16). To determine whether 17D and Asibi enter cells via CME, experiments were performed in HeLa cells depleted of clathrin heavy chain (CHC), a core component of CME (17). ATP6V1B2-depleted cells were used as positive controls. ATP6V1B2 is a subunit of the ATPase pump involved in endosome acidification and is therefore required for fusion of flavivirus envelope with endosomal membranes (18). Small interfering RNA (siRNA)-mediated silencing of CHC or ATP6V1B2 resulted in strong repression of target proteins compared to control siRNA (see Fig. S2A in the supplemental material). Additionally, HeLa cells transfected with CHC siRNA displayed accumulation of the transferrin receptor CD71 at the cell surface (see Fig. S2B) and strong inhibition of clathrin-mediated uptake of transferrin (see Fig. S2C). Next, CHC- or ATP6V1B2-depleted HeLa cells were challenged for 24 h with the vaccine or the parental YFV strain. WNV was used as control virus since its entry is mediated by a clathrin-dependent mechanism (18, 19). Immunofluorescence analysis performed with appropriate anti-E protein Ab showed that ATP6V1B2 knockdown potently inhibited WNV, Asibi, and 17D infection (Fig. 2A), indicating that both WNV entry and YFV entry are mediated by a pH-dependent fusion mechanism. As expected, CHC knockdown potently inhibited WNV infection, confirming previous findings (18, 19). Similarly, the Asibi YFV strain failed to infect CHC-depleted HeLa cells (Fig. 2A), demonstrating that Asibi infection requires a functional CME pathway. In marked contrast, 17D productively infected HeLa cells depleted of CHC and unable to take up ligands by CME (Fig. 2A). Similar results were obtained using siRNA targeting the mu subunit of the AP2 complex, a component of clathrin-coated pits (see Fig. S2D). To strengthen these observations, viral RNA amplification was quantified in CHC- and ATP6V1B2-depleted HeLa cells infected for 12 h with WNV, 17D, or Asibi (Fig. 2B). Viral RNA production was greatly affected by ATP6V1B2 silencing in cells infected with any of the 3 viruses (Fig. 2B). A strong repression of Asibi and WNV RNA amplification was observed in CHC-depleted cells (Fig. 2B), while 17D replication was not affected (Fig. 2B). Similar results were obtained using 17D or Asibi YFVs derived from molecular clones (see Fig. S2E). To rule out the possibility that differences in the virus input might influence the mechanism of entry, CHC-depleted cells were infected with 17D or Asibi at various MOI. Analysis of the number of cells positive for 17D or Asibi E

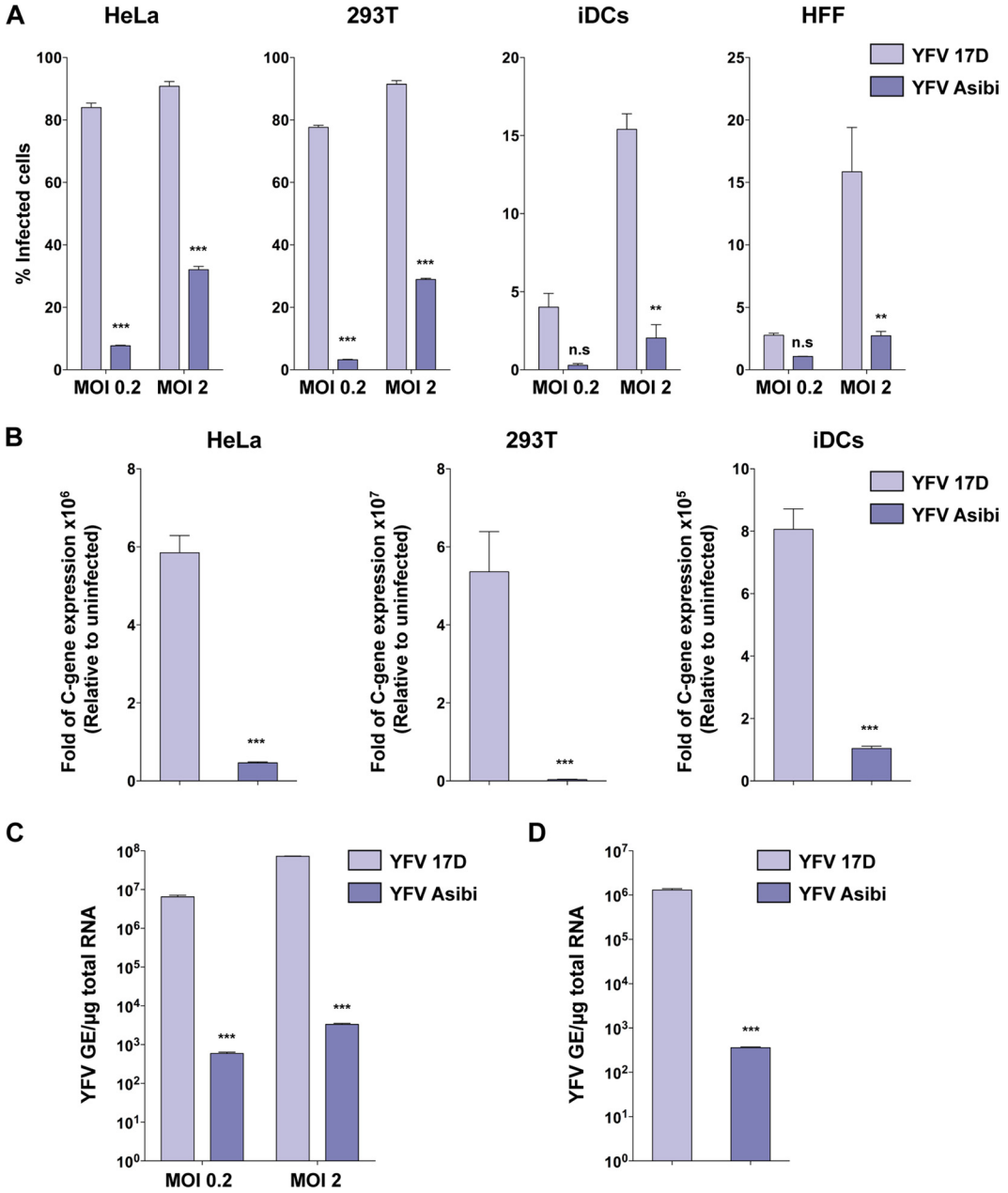

FIG 1 The 17D vaccine binds and infects human cells more efficiently than the parental strain Asibi. (A) HeLa and 293T cells, primary immature dendritic cells (iDCs), and human foreskin fibroblasts (HFFs) were infected with YFV 17D or Asibi at an MOI of 0.2 or 2. Twenty-four hours after infection, the percentage of infected cells was assessed by flow cytometry using the 2D12 anti-YFV E protein MAb. The data shown are means ± SD from three independent experiments (n.s, nonsignificant; **, $P < 0.001$; ***, $P < 0.0001$). (B) HeLa and 293T cells and iDCs were either mock infected or infected with YFV 17D or Asibi (MOI of 2), and total cellular RNA was extracted 8 h postinfection. Relative viral RNA levels were determined by real-time quantitative PCR (RT-qPCR) with human GAPDH as an endogenous control. Results are expressed as fold difference using expression in uninfected cells as the calibrator value. The data shown are representative of three independent experiments performed in triplicate (***, $P < 0.0001$). (C) Indicated MOI of the YFV 17D and Asibi strains were absorbed on HeLa cells for 1 h at 4°C. Total RNA was extracted, and quantitative PCR was performed to determine the amount of bound viral particles. (D) The YFV 17D and Asibi strains (MOI of 10) were absorbed on HeLa cells for 1 h at 4°C. Internalization was initiated by shifting cells to 37°C, and 2 h later, cells were treated with proteinase K (1 mg/ml) at 4°C for 45 min. Total RNA was extracted, and quantitative PCR was performed to determine the amount of YFV viral RNA molecules internalized. Alternatively total RNA was extracted from cells kept at 4°C after viral absorption and similarly treated with proteinase K. Results are expressed after subtraction of the YFV RNA level quantified in cells kept at 4°C from the YFV RNA level quantified in cells shifted at 37°C. (C and D) Amounts of viral RNA are expressed as genome equivalents (GE) per microgram of total cellular RNA. The data shown are representative of two independent experiments performed in duplicate (***, $P < 0.0001$).

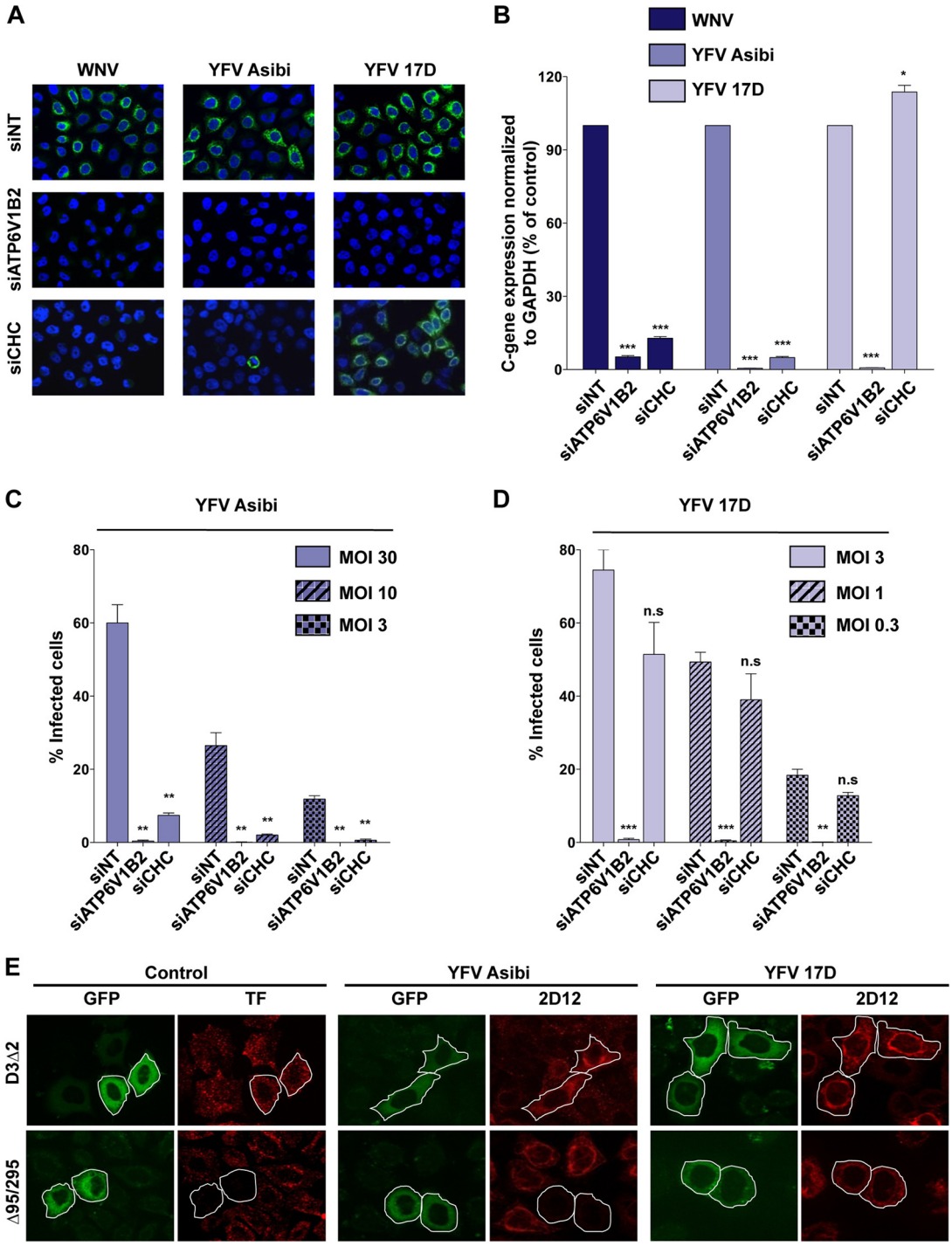

FIG 2 YFV Asibi and 17D use distinct endocytotic routes for entry. (A and B) HeLa cells were transfected with an siRNA pool targeting the clathrin heavy chain (siCHC) or ATP6V1β2 or a nontargeting siRNA (siNT) as a negative control and then infected with Asibi (MOI of 30) or 17D (MOI of 1) at 72 h posttransfection. (A) The next day, infection was assessed by immunofluorescence using the 2D12 anti-YFV E protein MAb or the E16 anti-WNV E protein MAb. The data shown are representative of two independent experiments. (B) Total RNA was extracted from infected cells 24 h postinfection, and viral RNA levels were determined by RT-qPCR with human GAPDH as the endogenous control. Results are expressed as the fold difference using expression in siNT-transfected cells as the calibrator value. The data shown are representative of three independent experiments performed in triplicate (*, $P < 0.01$; ***, $P < 0.0001$). (C and D) siRNA-transfected cells were challenged with the indicated MOI of 17D or the Asibi strain, and infection was assessed 24 h later by flow cytometry using the anti-YFV E 2D12 MAb. The data shown are representative of three independent experiments performed in duplicate (n.s, nonsignificant; **, $P < 0.001$; ***, $P < 0.0001$). (E) Effect of DN Eps15 mutant overexpression on YFV infection. HeLa cells were transfected with plasmids expressing the EGFP-Eps15 DN (Δ95/295) mutant or EGFP-Eps15 control mutant (D3Δ2). Cells expressing the transgenes were detected by GFP expression (green). Transferrin uptake was assessed 48 h posttransfection by incubating serum-starved cells for 10 min with Alexa Fluor 555-labeled human transferrin (red). Alternatively, cells expressing GFP-Eps15 mutants were infected with YFV Asibi (MOI of 30) or the 17D strain (MOI of 1) 48 h posttransfection. Infected cells were stained 24 h postinfection with anti-E 2D12 MAb followed by anti-mouse Alexa Fluor 594 (red). The data shown are representative of three independent experiments.

protein revealed that regardless of the viral input, the vaccine and virulent YFV strains displayed a different clathrin requirement for infection (Fig. 2C and D).

Eps15 is a protein involved in clathrin-coated vesicle assembly (20). Overexpression of dominant-negative (DN) mutant of Eps15 (Δ95-295) inhibits CME (20). To further investigate the requirement of CME during YFV infection, HeLa cells expressing green fluorescent protein (GFP) fused to the DN Δ95-295 mutant or, as a control, the functional mutant D3Δ2, were infected with either the parental or vaccine strain for 24 h. Expression of the DN form of Eps15, but not the control mutant D3Δ2, inhibited the internalization of transferrin (Fig. 2E), validating the functionality of the two mutants in our experimental system. Asibi infection was blocked in cells expressing DN Eps15 (Fig. 2E), consistent with a major role of CME in Asibi entry (Fig. 2A to D). In contrast, DN Eps15 expression had no effect on 17D infection (Fig. 2E), further demonstrating that the vaccine strain entry occurs in the absence of clathrin-coated vesicles. Similar results were obtained when HeLa cells were transfected with an siRNA targeting Eps15 (see Fig. S2F in the supplemental material). Together, our data reveal that, in contrast to Asibi, 17D enters target cells in a clathrin-independent manner.

Characterization of the clathrin-independent pathway used by 17D. Clathrin-independent endocytosis can be classified based on the utilization of dynamin-2 (DYN2), a large GTPase involved in pinching of endocytic vesicles from the plasma membrane (21). Several approaches were used to establish whether the 17D endocytic mechanism requires DYN2-dependent vesicle scission. First, RNA interference (RNAi)-mediated silencing was exploited to reduce DYN2 expression in HeLa cells (Fig. 3A, inset). The inhibitory effect of DYN2 silencing on endocytosis was confirmed by quantifying the amount of the transferrin receptor CD71 at the plasma membrane (see Fig. S3 in the supplemental material). DYN2-depleted cells were infected with 17D or Asibi for 24 h. These cells were refractory to infection with both viral strains (Fig. 3A). In a second strategy, HeLa cells were treated with different concentrations of the dynamin inhibitor dynasore (22) prior to virus infection. Dynasore treatment reduced the number of Asibi- and 17D-infected cells in a dose-dependent fashion (Fig. 3B). Finally, expression of the DN DYN2 K44A mutant fused to GFP was used to inhibit DYN2-mediated endocytosis (23). Infection by either 17D or Asibi was greatly reduced in cells expressing the K44A mutant compared to control cells (Fig. 3C). Together, these results demonstrate that both 17D and Asibi enter cells in a DYN2-dependent manner.

The caveolin-dependent endocytosis is the best characterized among the clathrin-independent, dynamin-dependent pathways (21, 24). To investigate the role of caveolae in 17D uptake, two different approaches were exploited. First, caveolin was depleted using a pool of siRNAs against caveolin-1 (Cav-1) (Fig. 3D, inset). Cav-1 depletion had no effect on 17D or Asibi infection (Fig. 3D). In a second approach, cells were transfected with a DN version of Cav-1 fused to GFP and infected with either 17D or Asibi virus. After 24 h, infection was assessed by immunofluorescence detection of the YFV E antigen. The expression of the Cav-1 DN mutant had no effect on either 17D or Asibi infection (Fig. 3E). Therefore, both YFV strains can efficiently infect cells devoid of caveolae. In sum, the parental strain Asibi, like other flaviviruses, enters HeLa cells in a clathrin-dependent manner. In contrast, 17D is internalized in HeLa cells in a clathrin-independent, dynamin-dependent, and caveola-independent pathway. We extended our findings to two other human cell lines (see Fig. S4A and S4B in the supplemental material). Depletion of CHC or Cav-1 had no effect on 17D infection in these cells. An siRNA targeting the YFV E protein served as a transfection control in these experiments (see Fig. S4B). In addition, our data also indicate that 17D entry is independent of Rac1, Pak1, Pak2, as well as the actin-related protein cortactin, which are known to regulate the clathrin-independent pathway involved in the interleukin-2 receptor β (IL-2Rβ) internalization (see Fig. S5 and Text S1 in the supplemental material).

YFVs traffic through early and recycling endosomes. We next investigated whether 17D and Asibi traffic to the same endocytic compartments for successful infection. Members of the Rab family of small GTPases are key regulators of endosomal maturation, tethering, fusion, and trafficking (25). More than 60 Rab proteins have been identified, each specifically associated with a particular type of endosome or intracellular pathway (25). For instance, Rab5 is associated with early endosomes, whereas Rab7 is enriched in late endosomes. Rab4 mediates fast and direct recycling of early endosomes to the plasma membrane, while Rab11 is enriched in perinuclear endosomes and mediates their slow endocytic recycling. The postendocytic itineraries of the 17D and Asibi strains were assessed using DN versions of Rab proteins expressed in HeLa cells. Rab DN mutants have proven to be powerful tools to study the intracellular trafficking of viruses (18, 26). Cells were transfected with GFP-tagged DN versions of Rab5, Rab7, Rab4, or Rab11 and were infected with YFV Asibi or 17D for 24 h. As found for other flaviviruses (18), expression of DN Rab5 significantly impaired both 17D infection and Asibi infection (Fig. 4). In contrast, expression of the Rab7 DN mutant did not affect the infectivity of the two viruses (Fig. 4), suggesting that they do not require transport to late endosomes for viral fusion. Similarly, Rab4 DN mutant overexpression did not impair 17D or Asibi infection (Fig. 4). Finally, expression of the Rab11 DN mutant significantly reduced infection of both the 17D and Asibi viruses (Fig. 4). These results suggest that both YFV strains require transport through Rab5- and Rab11-positive perinuclear recycling endosomes to establish a productive infection.

Amino acid changes within the YFV E protein alter the viral entry route. Comparison of the Asibi and 17D genomes revealed that, among the 10 viral proteins, the E glycoprotein is the most heavily mutated, harboring 12 amino acid changes (8) (Fig. 5A). Based on the key role of the E protein in virus entry, mutations in the 17D E protein might be major determinants in the choice of the internalization route. To investigate this, we generated YFV reporter virus particles (RVPs) by complementation of a subgenomic WNV replicon (encoding WNV nonstructural proteins and GFP) with a plasmid encoding YFV structural proteins (C, prM, and E) provided in *trans*. RVPs, which have been extensively used to study flavivirus infection, rely on the WNV replication machinery and are capable of only a single round of infection (27). Because no mutation has arisen in the 17D C protein during serial passage (8), Asibi and 17D RVPs differ only by 1 mutation in prM and 12 mutations in E protein. The functionality of RVPs to study 17D E protein-mediated events was validated by performing the RVP neutralization assay with control or anti-YFV polyclonal Ab. 17D RVP infection of Vero cells was blocked by up to 95% in the presence of anti-YFV polyclonal Ab (ascites YFV French neurotropic strain [FNV]), whereas the control Ab had no inhibitory

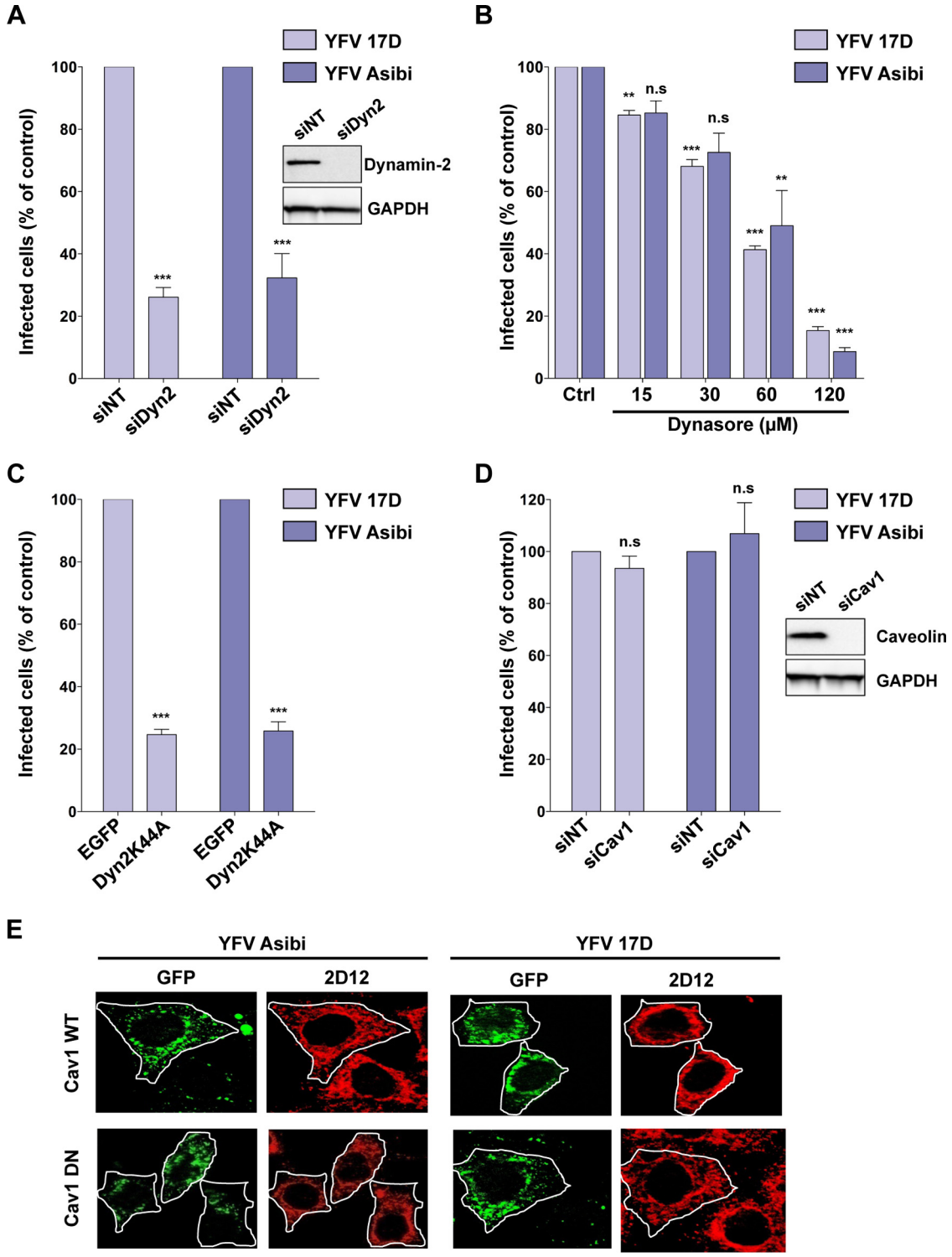

FIG 3 The 17D and Asibi entry pathways are dynamin dependent and caveolin-1 independent. (A) HeLa cells were transfected with an siRNA pool targeting dynamin-2 (siDyn2) or a nontargeting negative-control siRNA (siNT). Dynamin-2 expression was assessed 72 h posttransfection by immunoblotting (inset), and cells were infected with 17D (MOI of 1) or Asibi (MOI of 30). Infection was assessed 24 h later by flow cytometry using the 2D12 MAb and normalized to infection in siNT-transfected cells. The data shown are representative of three independent experiments performed in duplicate (***, $P < 0.0001$). (B) HeLa cells were pretreated with dynasore or vehicle (control [Ctrl]) for 30 min and then infected with 17D (MOI of 1) and YFV Asibi (MOI of 30) in the continuous presence of the drug. Infection was assessed 24 h later by flow cytometry using the 2D12 MAb and normalized to infection in control cells. (C) HeLa cells were transfected with an enhanced GFP (EGFP) backbone vector or the EGFP-dynamin-2 K44A mutant (Dyn2K44A). These cells were infected with 17D (MOI of 1) or Asibi (MOI of 30), and the infection level was assessed 24 h later by flow cytometry using the 2D12 anti-E MAb. (D) HeLa cells were transfected with an siRNA pool targeting caveolin-1 (siCav1) or a nontargeting negative-control siRNA (siNT). Caveolin-1 expression was assessed 72 h posttransfection by immunoblotting (inset). Alternatively, cells were infected with 17D (MOI of 1) or Asibi (MOI of 30). Infection was assessed 24 h later by flow cytometry using the 2D12 anti-E MAb

(Continued)

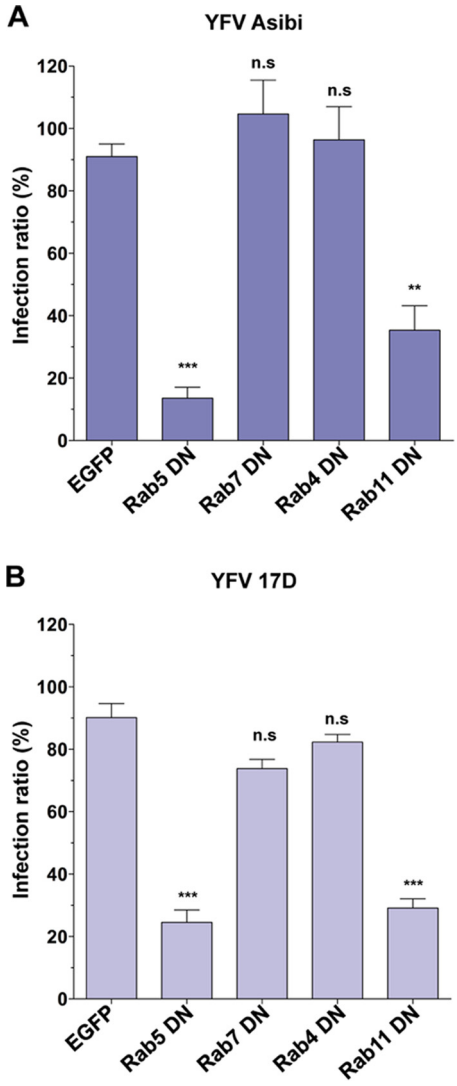

FIG 4 The 17D and Asibi strains traffic through early and recycling endosomes. HeLa cells were transfected with plasmids expressing EGFP fused to DN forms of Rab5, Rab7, Rab4, or Rab11 or with the EGFP backbone vector as a control. Cells were challenged 48 h postinfection with the Asibi (MOI of 30) (A) or 17D (MOI of 1) (B) strain. Infection was quantified 24 h later by flow cytometry using the 2D12 anti-E MAb. For each sample, the percentage of infected cells was quantified in an EGFP-negative and GFP-positive population. The effect of the EGFP-fusion protein on infectivity was expressed as the ratio of the infection level in GFP-positive cells to the infection level in the GFP-negative population. The data shown are representative of 3 independent experiments performed in duplicate (n.s, nonsignificant; **, $P < 0.001$; ***, $P < 0.0001$).

effect on infection (Fig. 5B). Forty hours following infection with 17D RVPs, between 12% and 50% of the cells were GFP positive, depending on the MOI and the cell types (Fig. 5C), further validating RVPs as a model system to study prM-E-mediated viral entry. Consistent with the results obtained in cells infected with replication-competent viruses (Fig. 1), we found that HeLa and 293T cells were more susceptible to 17D RVPs than to Asibi RVP infection (Fig. 5C). As expected from the experiments performed with infected cells (Fig. 2A to C), silencing of ATP6V1B2 reduced both Asibi and 17D RVP infections in HeLa cells (Fig. 5D). Moreover, depletion of CHC impaired Asibi RVP but not 17D RVP infection (Fig. 5D), demonstrating that the mutations present in 17D prM and/or E proteins are responsible for the change in the internalization mechanism. Only one mutation at position 36 has arisen in the prM protein during the attenuation process (L into F [Fig. 5A]) (8). Mutant 17D RVPs, in which the F was reversed to the parental L in prM, were generated (17DprM36FxL-RVPs). These mutant RVPs behaved like 17D RVP in term of sensitivity to CHC and ATP6V1B2 silencing (Fig. 5D). Altogether, these data indicate that the 12 mutations in the E protein are responsible for the clathrin-independent entry route used by the 17D vaccine strain. Interestingly, a mutation at position 380 in the E protein (E380) changed the Asibi TGD motif to an RGD integrin-binding motif in the 17D strain (8). The T-to-R substitution has been shown to increase the positive charge on the virion surface, which in turn accounts for an enhanced glycosaminoglycan binding capacity and reduced viral dissemination in the bloodstream (11). To investigate the impact of the E380 residue on YFV entry, we produced 17D and Asibi RVPs bearing the wild-type R or attenuated T residue at position E380, respectively (see Fig. S6 in the supplemental material). Asibi E380 T-to-R RVPs behaved like wild-type Asibi RVPs in terms of sensitivity to CHC silencing, indicating that the E380 R mutation is not a major determinant involved in the clathrin-independent entry of 17D (see Fig. S6). Unfortunately, we were unable to study the impact of the E380 R-to-T mutation on 17D entry. Indeed, 17D RVPs harboring this mutation were not released in the extracellular medium and failed to infect cells (data not shown).

17D entry leads to robust antiviral cytokine responses compared to wild-type Asibi virus. When exposed to viruses, most cells respond by producing IFNs of type I (IFN-α and IFN-β) and type III (IL-28A, IL-28b, and IL-29) (28). Secreted IFNs bind to their receptors and activate the canonical Jak/STAT pathway, leading to the expression of approximately 400 IFN-stimulated genes (ISGs) with antiviral properties (29), effectively establishing the antiviral state in infected and surrounding cells. Another prominent response to viral infection is the secretion of chemokines, which act mainly by attracting leukocytes to sites of viral infection. CXC-motif chemokine 10 (CXCL10), also known as IP-10, and C-C-motif chemokine ligand type 5 (CCL5), also known as Rantes, seem to be almost invariably associated with viral infections (30). To investigate a potential link between YFV entry and antiviral cytokine induction, we monitored the levels of IFN-β, IL-29, ISG56, CCL5, and CXCL10 transcripts in HeLa 293T cells, HFFs, and iDCs infected with 17D or Asibi for 24 or 48 h (Fig. 6A). 17D and Asibi RNA levels were assessed at these 2 time points, as well as 15 min postinfection to ensure that the inputs of cell-associated viral RNA were similar for both viral strains (Fig. 6A). These analyses revealed that cells infected with

Figure Legend Continued

and normalized to infection in siNT-transfected cells. (B to D) The data shown are representative of three independent experiments performed in duplicate (n.s, nonsignificant; **, $P < 0.001$; ***, $P < 0.0001$). (E) Representative immunofluorescence staining of HeLa cells transfected with the GFP-Cav1 WT or GFP-Cav1 DN mutant, infected 48 h posttransfection with the 17D (MOI of 1) or Asibi (MOI of 30) strain, and finally stained with anti-E 2D12 Ab (red).

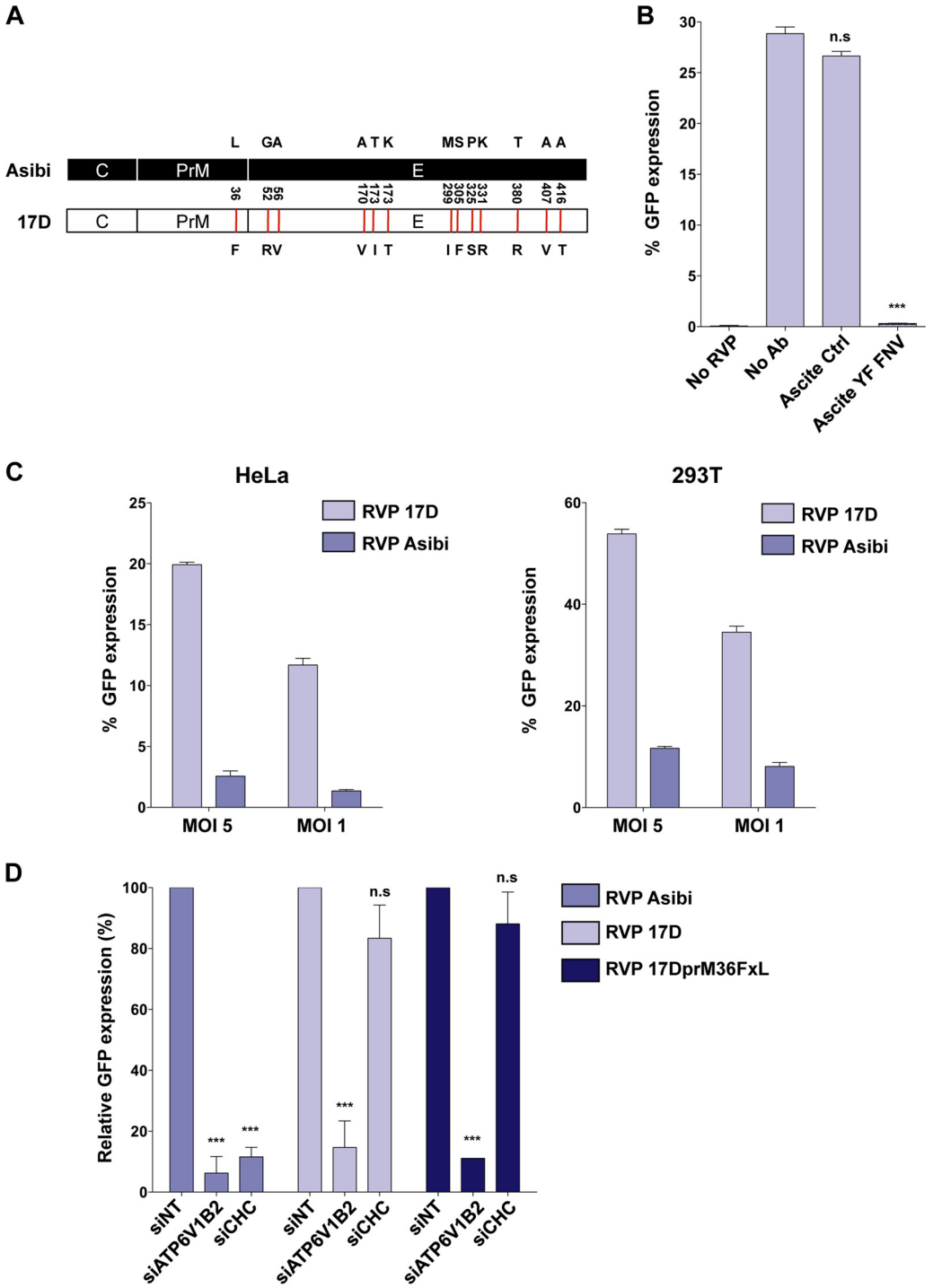

FIG 5 Amino acid changes within the YFV E protein alter the viral entry route. (A) Schematic representation of YFV Asibi (black) and 17D (white) structural proteins. Mutations found in 17D structural proteins are represented as red lines. (B) HeLa cells were challenged with 17D RVPs in the presence of YFV neutralizing Ab (ascites YF FNV) or control Ab. The percentage of GFP-positive cells was assessed 48 h later by flow cytometry. (C) 17D and Asibi RVPs show different infection profiles. The HeLa and 293T cell lines were infected with 17D or Asibi RVPs at the indicated MOI. The percentage of GFP-positive cells was assessed 48 h later by flow cytometry. (D) HeLa cells were transfected with an siRNA pool targeting the clathrin heavy chain (siCHC) or ATP6V1β2 or a control siRNA (siNT) and challenged 72 h posttransfection with 17D or Asibi RVPs. Alternatively, cells were infected with 17D RVPs exhibiting 1 amino acid change in the prM protein (RVP 17DprM36FxL). The percentage of GFP-positive cells was assessed 48 h later by flow cytometry and normalized to infection in siNT-transfected cells. (B to D) The data shown are representative of three independent duplicate experiments (n.s, nonsignificant; **, $P < 0.001$; ***, $P < 0.0001$).

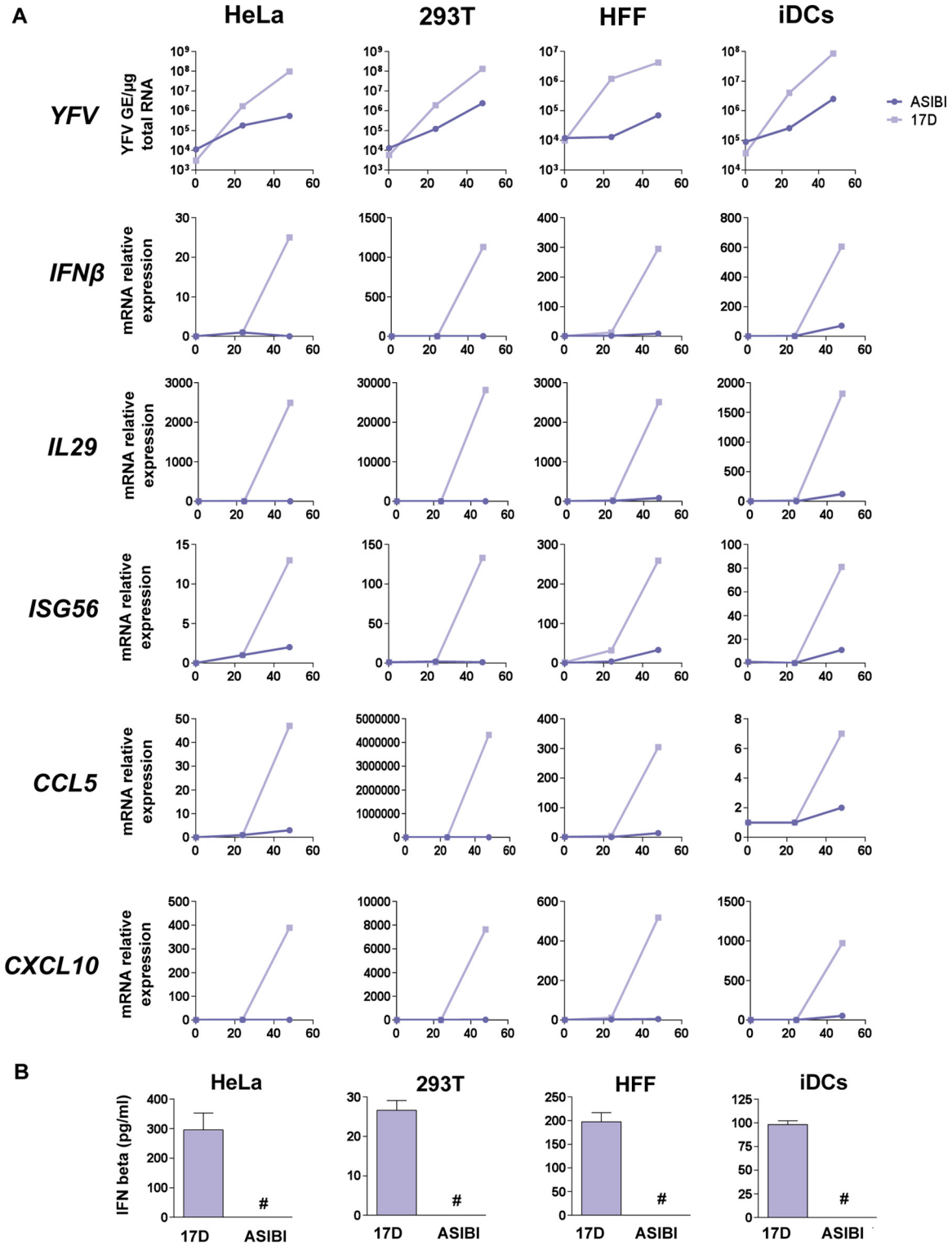

FIG 6 Comparison of the cytokine responses induced upon infection by 17D and Asibi. HeLa and 293T cells, human foreskin fibroblasts (HFFs), and primary immature dendritic cells (iDCs) were infected with 17D or YFV Asibi at an MOI of 2. (A) The relative amounts of cell-associated viral RNA and IFN-β, IL-29, ISG56, CCL5, and CXCL10 mRNAs were determined by qPCR analysis at 15 min, 24 h, and 48 h postinfection. Amounts of viral RNA are expressed as genome equivalents (GE) per microgram of total cellular RNA. All results are expressed as fold increases relative to uninfected cells. (B) Cell culture medium was analyzed by ELISA to determine the amounts of IFN-β secreted by the indicated cells. Values below the limit of detection of the IFN-β ELISA (12.5 pg/ml) are indicated by #. The data shown are representative of three independent experiments.

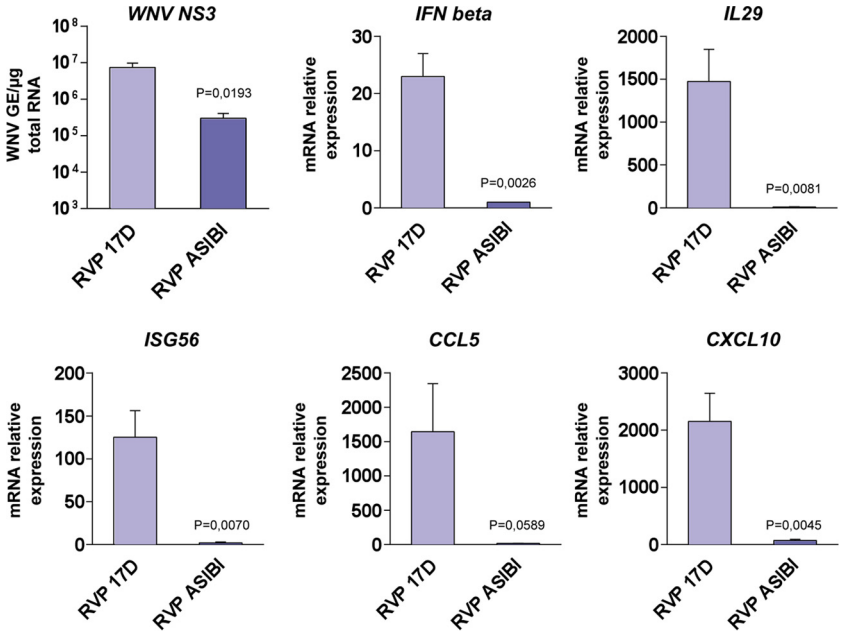

FIG 7 YFV entry mechanisms impact the activation of the cytokine-mediated antiviral response. 293T cells were challenged with 17D or Asibi RVPs at a MOI of 2. The relative amounts of cell-associated viral RNA and IFN-β, IL-29, ISG56, CCL5, and CXCL10 mRNAs were determined by RT-qPCR analysis at 48 h postinfection. The amounts of viral RNA are expressed as genome equivalents (GE) per microgram of total cellular RNA. All results are expressed as fold increases relative to uninfected cells. The data shown are representative of three independent experiments.

17D produced 1 to 2 log more viral RNA than cells infected with the parental Asibi strain (Fig. 6A), corroborating our previous findings (Fig. 1). The levels of IFN-β, IL-29, ISG56, CCL5, and CXCL10 transcripts were higher in 17D than in Asibi-infected cells in these 4 cell types (Fig. 6A). Consistently, between 25 and 300 pg/ml of IFN-β were secreted by cells infected with 17D, but IFN-β was undetectable in the supernatant of cells infected with similar amounts of Asibi (Fig. 6B).

To demonstrate that these differential cytokine responses are linked to the entry mechanisms of virulent and vaccine viruses, the levels of IFN-β, IL-29, ISG56, CCR5, and CLC10 transcripts were analyzed in 293T cells infected with 17D and Asibi RVPs (Fig. 7). As mentioned above, Asibi and 17D RVPs differ only by the type of incorporated E protein, both relying on the WNV replicon for their replication. As seen in cells infected with replication-competent viruses (Fig. 6A), cells challenged with 17D RVPs produced around 15 times more viral RNA than cells infected with Asibi RVPs (Fig. 7). The levels of transcripts of the five cytokines tested were higher in cells infected with 17D RVPs than those in cells infected with Asibi RVPs (Fig. 7). Together, these data show that the 17D entry mechanism correlates with a more robust cytokine-mediated antiviral response than that of Asibi.

DISCUSSION

By bringing the first evidence that vaccine and parental strains of YFV enter cells via distinct mechanisms and differentially stimulate the cytokine response, our study provides novel insights into YFV biology and the molecular determinants involved in attenuation of the widely used 17D vaccine.

The 17D strain is one of the most effective live attenuated vaccines ever generated; however, the molecular bases underlying virulence attenuation and immunogenicity are poorly understood. Genome comparison of parental Asibi and 17D viruses revealed that the E protein accumulated the largest number of mutations during the attenuation process (8), suggesting that it plays an essential role in YFV pathogenicity. Changes within the YFV E protein resulted in an alteration in its antigenicity and have been suspected to affect the mechanisms of YFV entry into target cells (8–11). In this study, we found that 17D binds to and enters target cells more efficiently than Asibi. Using expression of DN versions of proteins involved in endocytosis and RNA silencing strategies, our work reveals that 17D and Asibi use different endocytic pathways to infect target cells. Parental Asibi exploits the clathrin-mediated endocytosis, the major entry route used by flavivirus for internalization (16). In contrast, the vaccine strain 17D hijacks a clathrin- and caveolin-independent but dynamin-dependent pathway for productive infection. Clathrin-independent entry has been reported to mediate the internalization of a variety of unrelated viruses, including influenza virus in HeLa cells (31), rhesus rotavirus in MA104 cells (32), human rhinovirus 14 in rhabdomyosarcoma cells (33), serotype 2 of DV in Vero cells (34), and the vaccine strain of Japanese encephalitis virus in neuronal cells (35). We have further characterized the 17D entry pathway to be independent of Rac1, Pak1, and cortactin, which are crucial host factors involved in the clathrin-independent endocytosis of IL-2Rβ (36, 37). An in-depth analysis of the molecular signature of this nonclassical endocytic pathway is needed to better understand the early events of YFV 17D infection.

The experiments we conducted with YFV RVPs demonstrated that the 12 mutations differentiating the Asibi from the 17D E protein, which arose during attenuation (8), are responsible for the switch from a clathrin-dependent to a clathrin-independent internalization mode. Further studies are required to define which of the 17D mutations are sufficient for clathrin-independent entry. Interestingly, 5 out of 12 mutations found in YFV 17D glyco-

protein lie in domain III, which is believed to harbor the receptor-binding site (8). Amino acid changes in this region have been previously linked to E protein conformation changes and the modulation of YFV virulence in mice (10, 11). One can speculate that 17D and Asibi exploit distinct cellular receptors that are internalized via different pathways. This notion is supported by previous studies on measles virus showing that parental strains use the signaling lymphocyte activation molecule (SLAM) as the entry receptor, whereas the vaccine and laboratory-adapted measles virus strains, following amino acid substitutions in the envelope proteins, exploit CD46 as an alternate cellular receptor (38). Interestingly, mutation of the T residue at position 380 in domain III of the Asibi E protein into R creates an RGD motif in the 17D E protein. RGD motifs are binding sites for integrins (39). Although this motif is present in all three yellow fever vaccine viruses (17D-204, 17DD, and 17D-213) but absent both in the parental Asibi strain and in 22 additional WT YFV strains (40), its role in viral attenuation remains an open question. The finding that 17D infection is not affected by RGD-containing peptides or specific anti-integrin antibodies in primary dendritic cells (41, 42) seems to exclude a role for RGD-mediated integrin binding in 17D entry. Our data are consistent with this since E380 T-to-R change does not alter the YFV entry route. The R residue at position 380 in the 17D E protein is also a part of heparan sulfate (HS) binding domain, which seems to impact virus spread and attenuation (11, 43, 44). The acquisition of high HS-binding affinity following serial propagation in tissue culture appears to be a common mechanism for virulence attenuation of many viruses, including flaviviruses (45–52). It is plausible that increased affinity of 17D to glycosaminoglycan receptors contributes to the enhanced virus replication that we observed in several human cells. Interestingly, some glycosaminoglycan receptors traffic through a clathrin- and caveolin-independent, dynamin-dependent mechanism and associate with flotillin-1-positive vesicles (53). Therefore, one can speculate that 17D binds to heparan sulfate proteoglycans (HSPGs) and follows this unusual pathway for infectious entry.

Based on the correlation between virus entry and attenuation, we hypothesize that the infection by parental and vaccine YFV strains could impact the amplitude of the cellular antiviral response. Our data show that both replication-competent 17D viruses and RVPs harboring the 17D E protein induce higher expression of IFN-responsive genes and chemokines than their Asibi counterparts. More importantly, IFN-β secretion was readily detectable in several cellular systems following 17D but not Asibi infection, indicating that E protein-mediated events modulate the amplitude of the immune responses against YFV. Replication-competent 17D viruses bind to target cells more efficiently than Asibi viruses and also display an enhanced viral replication. One can speculate that increased 17D binding allows a more efficient delivery of 17D RNA into the cytoplasm, which in turn might activate the pattern recognition receptors (PRRs) and mediates a robust antiviral response. Changing the viral entry route, therefore, might happen as a result of change in virus receptor usage but may not be the main reason leading to an enhanced cytokine response. Additionally, it is plausible that virus uptake through this clathrin-independent pathway allows more efficient viral delivery into the endosomal compartment or protection of incoming virions from degradation as opposed to the classical clathrin-mediated route. Our results suggest that, despite being internalized by different routes, both Asibi and 17D traffic through early and recycling endosomes and are therefore likely to encounter the same PPRs. Recognition of 17D RNA by RIG-I, MDA5, and Toll-like receptor 7 (TLR7) has been reported in both immune and nonimmune cells *in vitro* (12, 54, 55), and it is highly plausible that these PPRs are also engaged by the parental Asibi strain. Overall, our data suggest that the difference in innate immune responses we observed correlates with the quantity of viral RNA delivered into infected cells, which itself is linked to the entry pathway used.

The stronger replication and subsequent increased antiviral responses observed in a panel of human cells infected by 17D could explain both the low viremia and rapid viral clearance observed in vaccinated subjects (12), as well as the loss of neurotropism and viscerotropism described in vaccinated nonhuman primates (4). Therefore, enhanced replication in the early phase of infection may be a feature of 17D attenuation. In contrast, infecting cells less efficiently, Asibi might replicate at lower levels in cells at the forefront of infection, passively escaping the detection of the innate immune sensors. This would allow the virus to disseminate and reach its target organs.

Our experiments conducted with 17D and Asibi RVPs suggest that the entry mechanisms account for most of the differences in cytokine response observed in 17D- or Asibi-infected cells. However, 17D attenuation is likely a multifactorial process that relies on additional mechanisms. For instance, flaviviruses, like many RNA viruses, encode viral proteins that antagonize antiviral signal transduction (56). Asibi is likely to express at least a protein with such properties, while the 17D counterpart might have lost this ability during the attenuation process. The nonstructural protein NS2A is a potential candidate since it exhibits the second highest number of amino-acid mutations (8). Another parameter that might contribute to 17D attenuation is the loss of genetic diversity (57); a phenomenon that has already been described for poliovirus (58). Whether all of these mechanisms are linked to virus entry and/or the activation of the antiviral response awaits further investigation.

MATERIALS AND METHODS

Cell lines. Cells of the HelaMZ (gift from L. Pelkmans, University of Zurich, Switzerland), human embryonic kidney 293T (American Type Culture Collection; ATCC), Vero (ATCC), and human hepatocarcinoma Huh7 and Huh7.5 (gifts from E. Meurs, Pasteur Institute, Paris, and C. Rice, Rockefeller University, NY, respectively) lines were maintained in Dulbecco's modified Eagle's medium (DMEM; Invitrogen) supplemented with 10% heat-inactivated fetal bovine serum (FBS) and 1% penicillin–streptomycin (P/S). Human foreskin fibroblasts (HFFs) (gift from C. Neuveut, Pasteur Institute, Paris) were maintained in DMEM supplemented with 8% FBS plus 1% P/S. Hep2 cells stably expressing IL-2Rβ, designated Hep2β (36), were grown in DMEM supplemented with 10% FBS and 1.5 mg/ml of geneticin (Gibco). The hepatocellular carcinoma HepG2 cells (gift from C. Neuveut, Pasteur Institute, Paris) were maintained in DMEM–F-12 (Invitrogen) supplemented with 10% FBS, 1% P/S, 0.2 μg/ml of hydrocortisone (Sigma), and 5 μg/ml of insulin (Sigma). Baby hamster kidney cells (BHK-21; National Reference Centre for Arboviruses, Pasteur Institute, Paris) were cultured in Glasgow's modified Eagle's medium (GMEM) supplemented with 5% FBS, 10% tryptose phosphate, and 1% P/S. Dendritic cells were generated by differentiation of human monocytes as previously described (59). C6/36 *Albopictus* mosquito cells (National Reference Centre for Arboviruses, Pasteur Institute, Paris) were cultured in Leibovitz's L-15 medium supplemented with 10% FBS, 1% P/S, tryptose phosphate broth, and nonessential amino acids.

Ethics statement. Blood from healthy adult donors was provided by Etablissement Français du Sang (EFS), Paris, France, within the frame-

work of a bilateral agreement between EFS and Hôpital Saint-Louis or the Pasteur Institute, All samples were anonymized and collected in accordance with EU standards and national laws.

Plasmids. pACNR-113.16 plasmid containing the full-length infectious YFV Asibi genome under an SP6 promoter was provided by C. M. Rice (Rockefeller University, NY). The pACNR-FLYF17DII plasmid expressing the full-length infectious 17D genome was a gift from P. Bredenbeek (Leiden University Medical Center, the Netherlands) (60). The plasmids encoding a subgenomic GFP-Zeocin replicon and structural genes (C, prM, and E) of the lineage II strain of WNV (strain WN 956 D117 3B) were provided by T. C. Pierson (NIH, Bethesda, MD) (61). Plasmids expressing control and DN forms of Eps15 were a gift from A. Dautry-Varsat (Pasteur Institute, France) (20). Vectors encoding Cav1 and Dynamin-2 WT and corresponding DN mutant versions were a gift from A. Helenius (ETH Zurich, Switzerland) (62). GFP-tagged DN forms of Rab5, Rab7, Rab4, or Rab11 were previously described (63). YFV Asibi and 17D C, prM, and E genes were amplified by PCR from the pACNR-113.16 and pACNR-FLYF17DII plasmids, respectively, and were cloned as BamHI- and XhoI-digested fragments into a likewise pcDNA3.1-digested plasmid. pcDNA3-YFV17D-prM36FxL was engineered by site-directed mutagenesis on the pcDNA3-YFV17D-CprME plasmid using the sense primer 5′-ATT GAG AGA TGG CTG GTG AGG AAC C and antisense primer 5′-G GTT CCT CAC CAG CCA TCT CTC AAT. pYF17D-GFP was derived from pACNR-FLYF17DII. Briefly, a BspE1 restriction site was introduced downstream of the stop codon of the YFV17D polyprotein. The internal ribosome entry site (IRES) AcGFP cassette was amplified from pIRES2-AcGFP1 (Clontech) with primers containing a BspE1 restriction site and introduced into pACYC-YFV17D.

Antibodies and reagents. Antibodies were as follows: anti-transferrin receptor CD71 conjugated with phycoerythrin (PE) (clone YDJ1.2.2; Beckman Coulter), mouse control isotype IgG1 (BD Biosciences), mouse anti-human clathrin heavy chain (Abcam), rabbit anti-human dynamin-2 (Interchim), rabbit anti-human ATP6V1β2 (Abcam), mouse anti-human caveolin-1 (Santa Cruz), rabbit anti-human Pak1 (Santa Cruz), rabbit anti-human Rac1 (Santa Cruz), mouse anti-human cortactin (Santa Cruz), antitransferrin conjugated with Alexa Fluor 555 (Life Technologies), mouse anti-human GAPDH (glyceraldehyde-3-phosphate dehydrogenase) (Abcam), fluorescein isothiocyanate (FITC), or Texas Red-conjugated goat anti-mouse IgG (Dako, CA, United States), and anti-mouse or anti-rabbit horseradish peroxidase (HRP)-coupled secondary antibodies (Agilent Technologies). The anti-IL-2 receptor β-chain monoclonal antibody 561 was previously described (64). Mouse anti-E protein 2D12 were produced from the hydridoma cell line ATCC CRL-1689. Mouse anti-E 4G2 and ascites from mice inoculated with the French neurotropic (FNV) strain of YFV were produced by RD Biotech, France. E16 anti-WNV E was previously described (65). Dynasore (Sigma-Aldrich D7693) was used at the indicated concentration by treating the cells 30 min prior to infection. In these experiments, dimethyl sulfoxide (DMSO) was used as a control treatment.

Virus preparation and titration. Vaccine 17D YFV (Stamaril vaccine; Sanofi Pasteur, Lyon, France) was provided by the Pasteur Institute Medical Center. WT Asibi YFV and WNV (Israeli strain IS-98-STI) were provided by the Biological Resource Center of Institut Pasteur. 17D and Asibi stocks were prepared on Vero cells and titrated on Vero cells by plaque assay as previously described (66). WNV was propagated on C6/36 cells. YFV stocks were concentrated by polyethylene glycol 6000 precipitation and purified by centrifugation in a discontinued gradient of sucrose. Sucrose-purified viruses were used for the experiments presented in Fig. 6. For the experiments shown in Fig. S1E in the supplemental material, 17D and Asibi stocks were generated from their respective molecular clones, as previously described (60). Briefly, plasmid DNA was linearized with restriction enzyme XbaI, recovered by phenol-chloroform extraction and ethanol precipitation, and used as the templates for *in vitro* transcription using the mMessage mMachine transcription kits (Ambion). *In vitro*-synthesized RNA transcripts were purified *in vitro* using the RNeasy kit (Qiagen), extracted with phenol-chloroform, precipitated with sodium acetate and ethanol, washed with 70% ethanol, and resuspended in RNase-free water. The resulting RNA was transfected into BHK-21 cells using Lipofectamine 2000. Virus-containing medium was harvested 2 days posttransfection.

siRNA transfections and virus infection assays. Cells were transfected using the Lipofectamine RNAiMax protocol (Life Technologies) with 30 nM final concentrations of siRNAs following the manufacturer's protocol. After 72 h, cells were infected at the indicated MOI, and infection was quantified by flow cytometry or analyzed by immunofluorescence. Pools of siRNAs (ON-TARGETplus SMARTpool) were obtained from Dharmacon: clathrin heavy chain (CHC) (L019856-00), dynamin-2 (L-004007-00), human ATP6V1B2 (L-011589-01), human caveolin (L-003467-00), human Pak1 (L-003521-00), human Rac1 (L-003560-00), human cortactin (L-010508-00), human EPS15 (L-004005-00), human AP2M1 (L-008170-00), and a nontargeting negative control (NT) (D-001810-10). The siRNA targeting the E protein of YFV has been previously described (67).

Flow cytometry assays. Flow cytometry analysis was performed as previously described (68). WNV infection was detected using the pan-flavivirus 4G2 anti-E monoclonal antibody (MAb). YFV infection was detected using the 2D12 anti-E MAb.

Analysis of transferrin receptor (CD71) cell surface expression. HeLa cells were washed once in PBS and were detached by incubation with PBS-EDTA. After 10 min of saturation in buffer (PBS, 1% bovine serum albumin [BSA]), cells were incubated at 4°C for 45 min with phycoerythrin (PE)-conjugated CD71 MAb. After extensive washing with the PBS-BSA buffer, cells were fixed with 4% paraformaldehyde (PFA) in PBS for 20 min at room temperature before being subjected to flow cytometry analysis. PE-conjugated IgG1 Ab was used as the isotype control.

Western blot analysis. Cells were lysed in lysis buffer (1% 50 mM Tris-HCl, 150 mM NaCl, Triton X-100) in the presence of complete protease inhibitors (Roche Diagnostics, Basel, Switzerland) for 20 min at 4°C. Equal amounts of protein (determined by Bradford assay) were subjected to sodium dodecyl sulfate-polyacrylamide gel (4 to 12%) electrophoresis (Bio-Rad, Hercules, CA), followed by transfer onto a polyvinylidene difluoride (PVDF) membrane (Millipore, Billerica, MA). Various amounts of GAPDH were used as loading controls. Staining was revealed with corresponding horseradish peroxidase (HRP)-coupled secondary antibodies and developed using ECL Plus Western blotting detection reagents (Amersham) following the manufacturer's instructions. Image acquisition was performed by using an LAS-1000 charge-coupled device (CCD) camera and Image Gauge software version 4.22 (Fuji Photo Film Co).

Binding and internalization assays. HeLa cells were washed with PBS and detached by incubation with PBS-EDTA. After 30 min of saturation in binding buffer (RPMI, 3% BSA), cells were incubated for 1 h at 4°C with the 17D or Asibi strain in binding buffer. Cells were washed twice with cold binding buffer and once with PBS to remove unbound particles. Total RNA was extracted from cells. For internalization experiments, cells were chilled on ice prior to incubation with YFV for 1 h at 4°C. Cells were extensively washed with PBS to remove unbound viral particles. Virus internalization was initiated by shifting the cells to 37°C for 2 h. Alternatively, cells were kept for 2 h at 4°C to prevent virus internalization. Then the cells were washed with cold PBS and treated with proteinase K (1 mg/ml) (Life Technologies) for 45 min at 4°C. Proteinase K was inactivated by addition of 2 mM phenylmethylsulfonyl fluoride (PMSF) in PBS-BSA (3%), and detached cells were pelleted and washed in cold PBS-BSA (0.2%), and total RNA was extracted by using TRIzol (Life Technologies) to quantify the amount of internalized YFV RNA by qPCR. Genome equivalent (GE) concentrations were determined by extrapolation from a standard curve obtained with serial dilutions of the pACNR-113.16 plasmid.

RNA purification, reverse transcription, and quantitative real-time PCR. Total RNA was extracted from infected cells using a DNeasy kit (Qiagen) and treated with DNase (RNase-free DNase set from Qiagen).

Total cDNA was produced by reverse transcription (RT) of equal amounts of purified RNA (0.5 μg) using random primers (Roche) and SuperScript II reverse transcriptase (Invitrogen), according to the manufacturers' protocols. Samples were treated with RNase H (Biolabs). Genomic viral RNA was quantified by real-time qPCR on an ABI Prism 7300 sequence detection system using the SYBR green PCR kit according to the manufacturer's instructions (Applied Biosystems). The primers used for qPCR were designed with PrimerExpress 2.0 software (Applied Biosystems) and are listed in Table S1 in the supplemental material. Relative expression quantification was performed based on the comparative threshold cycle (C_T) method, using GAPDH as the endogenous reference control. Genome equivalent (GE) concentrations were determined by extrapolation from a standard curve obtained with serial dilutions of the pACNR-113.16 plasmid.

YFV RVP production and titration. Reporter virus particles (RVPs) were produced by a complementation approach as described previously (61). Briefly, 293T cells were transfected with a total of 4 μg of two different plasmids (3 μg of plasmid encoding structural proteins and 1 μg of replicon plasmid) per well in 6-well plates using Lipofectamine LTX (Invitrogen). Lipid-DNA complexes were replaced 5 h later with a low-glucose formulation of DMEM containing 10% FBS. RVP-containing medium was harvested 44 h posttransfection. RVPs were titrated on Vero cells infected for 48 h by measuring GFP expression by flow cytometry.

Immunofluorescence assays. HelaMZ cells were cultured on Lab-Tek II-CC^2 chamber slides (Nunc, Roskilde, Denmark). Samples were processed as described previously (69). Briefly, cells were fixed with 4% PFA and permeabilized with 1% saponin. Slides were mounted with ProLong Gold antifade reagent containing 4′,6-diamidino-2-phenylindole (DAPI) for nuclei staining. Samples were analyzed using an upright Zeiss Observer microscope system (Carl Zeiss, Jena, Germany) equipped with an ApoTome. z-series of 1-μm optical sections were acquired, and single optical sections through the cells are depicted. Image analysis was done with AxioVision imaging software version 4.4 (Carl Zeiss, Germany). Analyses were performed at least twice, and at least 100 cells were visualized.

For endocytosis quantification, Hep2β cells were incubated with transferrin coupled to Alexa Fluor 488 (TfA488, Molecular Probes) and anti-IL-2Rβ coupled to Cy3 for a time course up to 15 min at 37°C to allow receptor entry (70). The anti-IL-2Rβ antibody recognizes the extracellular part of IL-2Rβ and does not affect the binding of the ligand IL-2 or the traffic of the receptor (64). Cells were fixed and permeabilized as described above. To detect cell boundaries, cells were stained with HCS Cell mask Alexa Fluor 350 (Invitrogen Molecular Probes, 1.25 ng/ml). Images were obtained as described above and collected from at least three independent experiments, representing at least 100 cells. They were further analyzed and quantified using Icy software as previously described (70, 71).

Transferrin uptake assays. Cells were serum starved 1 h prior to incubation with Alexa Fluor 555-labeled human transferrin (Molecular Probes) diluted in DMEM (1/1,000) for 10 min at 37°C. Residual and noninternalized transferrin was removed by PBS washing, and cells were processed for immunofluorescence as described above.

ELISA. Cell culture supernatants were analyzed by enzyme-linked immunosorbent assay (ELISA) for total IFN-β using the Verikine human IFN-β multisubtype ELISA kit (PBL Assay Science, NJ) according to the manufacturer's instructions.

Statistical analyses. Graphical representation and statistical analyses were performed using Prism5 software (GraphPad Software). Unless otherwise stated, results are shown as means ± standard deviations (SD) from 3 independent experiments. Differences were tested for statistical significance using the one-way analysis of variance (ANOVA) test.

SUPPLEMENTAL MATERIAL

Supplemental material for this article may be found at http://mbio.asm.org/lookup/suppl/doi:10.1128/mBio.01956-15/-/DCSupplemental.

Text S1, DOCX file, 0.1 MB.
Figure S1, TIF file, 0.1 MB.
Figure S2, TIF file, 1.1 MB.
Figure S3, TIF file, 0.1 MB.
Figure S4, TIF file, 0.6 MB.
Figure S5, TIF file, 0.3 MB.
Figure S6, TIF file, 0.1 MB.
Table S1, TIF file, 0.2 MB.

ACKNOWLEDGMENTS

We thank L. Pelkmans for the HelaMZ cells, C. Rice for the Huh7.5 cells and the pACNR-113.16 plasmid, E. Meurs for Huh7 cells, C. Neuveut for the HepG2 cells and HFFs, P. Bredenbeek for the pACNR-FLYF17DII plasmid, A. Dautry-Varsat for Eps15 plasmids, A. Helenius for Cav1 and dynamin-2 vectors, and T. C. Pierson for the subgenomic WNV replicon and plasmids containing WNV structural genes. We are also thankful to Sandy Simon and Olivier Schwartz for critical reading of the manuscript.

This project was supported by grants from the Fondation pour la Recherche Médicale, the French National Research Agency (ANR) (ANR-10-IHUB-0002, ANR-12-JSV3-003-01, and "Investissements d'Avenir" program ANR-10-IHUB-0002), Ville de Paris EMERGENCES Program, Marie Curie International Reintegration program PCIG11-GA-2012-322060, the INTRAPATH program of the Marie Curie FP6 framework, the Pasteur Institute, the Institut Universitaire d'Hématologie, and the Institut National de la Sante et Recherche Médicale. M.D.F.-G. held a fellowship from Marie Curie and "La Caixa" Foundation. O.D. received a scholarship from the French Ministry of Research.

FUNDING INFORMATION

Ville de Paris Emergences program provided funding to Nolwenn Jouvenet. Marie Curie International Reintegration program provided funding to Nolwenn Jouvenet under grant number PCIG11-GA-2012-322060. Intrapath program of the Marie Curie FP6 framework provided funding to Ali Amara. Institut universitaire d'Hematologie provided funding to Ali Amara. La Caixa Foundation provided funding to Maria Dolores Fernandez-Garcia. French Ministry of Research provided funding to Ophélie Dejarnac. Institut Pasteur provided funding to Nolwenn Jouvenet. Agence Nationale de la Recherche (ANR) provided funding to Ali Amara under grant numbers ANR-10-IHUB-0002 and ANR-10-IHUB-0002. Agence Nationale de la Recherche (ANR) provided funding to Nolwenn Jouvenet under grant number ANR-12-JSV3-003-01. Institut National de la Sant et de la Recherche Mdicale (Inserm) provided funding to Ali Amara. Fondation pour la Recherche Mdicale (FRM) provided funding to Ali Amara.

REFERENCES

1. **Fernandez-Garcia MD, Mazzon M, Jacobs M, Amara A**. 2009. Pathogenesis of flavivirus infections: using and abusing the host cell. Cell Host Microbe **5**:318–328. http://dx.doi.org/10.1016/j.chom.2009.04.001.
2. **Lindenbach BD, Rice CM**. 2003. Molecular biology of flaviviruses. Adv Virus Res **59**:23–61. http://dx.doi.org/10.1016/S0065-3527(03)59002-9.
3. **Monath TP, Barrett AD**. 2003. Pathogenesis and pathophysiology of yellow fever. Adv Virus Res **60**:343–395. http://dx.doi.org/10.1016/S0065-3527(03)60009-6.
4. **Pulendran B**. 2009. Learning immunology from the yellow fever vaccine: innate immunity to systems vaccinology. Nat Rev Immunol **9**:741–747. http://dx.doi.org/10.1038/nri2629.
5. **Barrett AD, Teuwen DE**. 2009. Yellow fever vaccine—how does it work and why do rare cases of serious adverse events take place? Curr Opin Immunol **21**:308–313. http://dx.doi.org/10.1016/j.coi.2009.05.018.
6. **Monath TP**. 2005. Yellow fever vaccine. Expert Rev Vaccines **4**:553–574. http://dx.doi.org/10.1586/14760584.4.4.553.
7. **Pulendran B, Oh JZ, Nakaya HI, Ravindran R, Kazmin DA**. 2013. Immunity to viruses: learning from successful human vaccines. Immunol Rev **255**:243–255. http://dx.doi.org/10.1111/imr.12099.
8. **Hahn CS, Dalrymple JM, Strauss JH, Rice CM**. 1987. Comparison of the virulent Asibi strain of yellow fever virus with the 17D vaccine strain

derived from it. Proc Natl Acad Sci U S A **84:**2019–2023. http://dx.doi.org/10.1073/pnas.84.7.2019.
9. **Barrett AD, Monath TP, Cropp CB, Adkins JA, Ledger TN, Gould EA, Schlesinger JJ, Kinney RM, Trent DW.** 1990. Attenuation of wild-type yellow fever virus by passage in HeLa cells. J Gen Virol **71:**2301–2306. http://dx.doi.org/10.1099/0022-1317-71-10-2301.
10. **Sil BK, Dunster LM, Ledger TN, Wills MR, Minor PD, Barrett AD.** 1992. Identification of envelope protein epitopes that are important in the attenuation process of wild-type yellow fever virus. J Virol **66:**4265–4270.
11. **Lee E, Lobigs M.** 2008. E protein domain III determinants of yellow fever virus 17D vaccine strain enhance binding to glycosaminoglycans, impede virus spread, and attenuate virulence. J Virol **82:**6024–6033. http://dx.doi.org/10.1128/JVI.02509-07.
12. **Querec TD, Akondy RS, Lee EK, Cao W, Nakaya HI, Teuwen D, Pirani A, Gernert K, Deng J, Marzolf B, Kennedy K, Wu H, Bennouna S, Oluoch H, Miller J, Vencio RZ, Mulligan M, Aderem A, Ahmed R, Pulendran B.** 2009. Systems biology approach predicts immunogenicity of the yellow fever vaccine in humans. Nat Immunol **10:**116–125. http://dx.doi.org/10.1038/ni.1688.
13. **Wheelock EF, Sibley WA.** 1965. Circulating virus, interferon and antibody after vaccination with the 17-D strain of yellow-fever virus. N Engl J Med **273:**194–198. http://dx.doi.org/10.1056/NEJM196507222730404.
14. **Gaucher D, Therrien R, Kettaf N, Angermann BR, Boucher G, Filali-Mouhim A, Moser JM, Mehta RS, Drake DR, III, Castro E, Akondy R, Rinfret A, Yassine-Diab B, Said EA, Chouikh Y, Cameron MJ, Clum R, Kelvin D, Somogyi R, Greller LD, Balderas RS, Wilkinson P, Pantaleo G, Tartaglia J, Haddad EK, Sekaly RP.** 2008. Yellow fever vaccine induces integrated multilineage and polyfunctional immune responses. J Exp Med **205:**3119–3131. http://dx.doi.org/10.1084/jem.20082292.
15. **Lefeuvre A, Contamin H, Decelle T, Fournier C, Lang J, Deubel V, Marianneau P.** 2006. Host-cell interaction of attenuated and wild-type strains of yellow fever virus can be differentiated at early stages of hepatocyte infection. Microbes Infect **8:**1530–1538. http://dx.doi.org/10.1016/j.micinf.2006.01.013.
16. **Smit JM, Moesker B, Rodenhuis-Zybert I, Wilschut J.** 2011. Flavivirus cell entry and membrane fusion. Viruses **3:**160–171. http://dx.doi.org/10.3390/v3020160.
17. **McMahon HT, Boucrot E.** 2011. Molecular mechanism and physiological functions of clathrin-mediated endocytosis. Nat Rev Mol Cell Biol **12:**517–533. http://dx.doi.org/10.1038/nrm3151.
18. **Krishnan MN, Sukumaran B, Pal U, Agaisse H, Murray JL, Hodge TW, Fikrig E.** 2007. Rab 5 is required for the cellular entry of dengue and West Nile viruses. J Virol **81:**4881–4885. http://dx.doi.org/10.1128/JVI.02210-06.
19. **Chu JJ, Ng ML.** 2004. Infectious entry of West Nile virus occurs through a clathrin-mediated endocytic pathway. J Virol **78:**10543–10555. http://dx.doi.org/10.1128/JVI.78.19.10543-10555.2004.
20. **Benmerah A, Bayrou M, Cerf-Bensussan N, Dautry-Varsat A.** 1999. Inhibition of clathrin-coated pit assembly by an Eps15 mutant. J Cell Sci **112:**1303–1311.
21. **Mayor S, Pagano RE.** 2007. Pathways of clathrin-independent endocytosis. Nat Rev Mol Cell Biol **8:**603–612. http://dx.doi.org/10.1038/nrm2216.
22. **Macia E, Ehrlich M, Massol R, Boucrot E, Brunner C, Kirchhausen T.** 2006. Dynasore, a cell-permeable inhibitor of dynamin. Dev Cell **10:**839–850. http://dx.doi.org/10.1016/j.devcel.2006.04.002.
23. **Damke H, Baba T, Warnock DE, Schmid SL.** 1994. Induction of mutant dynamin specifically blocks endocytic coated vesicle formation. J Cell Biol **127:**915–934. http://dx.doi.org/10.1083/jcb.127.4.915.
24. **Mayor S, Parton RG, Donaldson JG.** 2014. Clathrin-independent pathways of endocytosis. Cold Spring Harb Perspect Biol **6:**a016758. http://dx.doi.org/10.1101/cshperspect.a016758.
25. **Stenmark H.** 2009. Rab GTPases as coordinators of vesicle traffic. Nat Rev Mol Cell Biol **10:**513–525. http://dx.doi.org/10.1038/nrm2728.
26. **Sieczkarski SB, Whittaker GR.** 2003. Differential requirements of Rab5 and Rab7 for endocytosis of influenza and other enveloped viruses. Traffic **4:**333–343. http://dx.doi.org/10.1034/j.1600-0854.2003.00090.x.
27. **Pierson TC, Sánchez MD, Puffer BA, Ahmed AA, Geiss BJ, Valentine LE, Altamura LA, Diamond MS, Doms RW.** 2006. A rapid and quantitative assay for measuring antibody-mediated neutralization of West Nile virus infection. Virology **346:**53–65. http://dx.doi.org/10.1016/j.virol.2005.10.030.
28. **Hoffmann HH, Schneider WM, Rice CM.** 2015. Interferons and viruses: an evolutionary arms race of molecular interactions. Trends Immunol **36:**124–138. http://dx.doi.org/10.1016/j.it.2015.01.004.
29. **Schoggins JW, Wilson SJ, Panis M, Murphy MY, Jones CT, Bieniasz P, Rice CM.** 2011. A diverse range of gene products are effectors of the type I interferon antiviral response. Nature **472:**481–485. http://dx.doi.org/10.1038/nature09907.
30. **Melchjorsen J, Sørensen LN, Paludan SR.** 2003. Expression and function of chemokines during viral infections: from molecular mechanisms to in vivo function. J Leukoc Biol **74:**331–343. http://dx.doi.org/10.1189/jlb.1102577.
31. **Sieczkarski SB, Whittaker GR.** 2002. Influenza virus can enter and infect cells in the absence of clathrin-mediated endocytosis. J Virol **76:**10455–10464. http://dx.doi.org/10.1128/JVI.76.20.10455-10464.2002.
32. **Sanchez-San Martin C, López T, Arias CF, López S.** 2004. Characterization of rotavirus cell entry. J Virol **78:**2310–2318. http://dx.doi.org/10.1128/JVI.78.5.2310-2318.2004.
33. **Khan AG, Pickl-Herk A, Gajdzik L, Marlovits TC, Fuchs R, Blaas D.** 2010. Human rhinovirus 14 enters rhabdomyosarcoma cells expressing ICAM-1 by a clathrin-, caveolin-, and flotillin-independent pathway. J Virol **84:**3984–3992. http://dx.doi.org/10.1128/JVI.01693-09.
34. **Acosta EG, Castilla V, Damonte EB.** 2009. Alternative infectious entry pathways for dengue virus serotypes into mammalian cells. Cell Microbiol **11:**1533–1549. http://dx.doi.org/10.1111/j.1462-5822.2009.01345.x.
35. **Kalia M, Khasa R, Sharma M, Nain M, Vrati S.** 2013. Japanese encephalitis virus infects neuronal cells through a clathrin-independent endocytic mechanism. J Virol **87:**148–162. http://dx.doi.org/10.1128/JVI.01399-12.
36. **Grassart A, Dujeancourt A, Lazarow PB, Dautry-Varsat A, Sauvonnet N.** 2008. Clathrin-independent endocytosis used by the IL-2 receptor is regulated by Rac1, Pak1 and Pak2. EMBO Rep **9:**356–362. http://dx.doi.org/10.1038/embor.2008.28.
37. **Basquin C, Malardé V, Mellor P, Anderson DH, Meas-Yedid V, Olivo-Marin JC, Dautry-Varsat A, Sauvonnet N.** 2013. The signalling factor PI3K is a specific regulator of the clathrin-independent dynamin-dependent endocytosis of IL-2 receptors. J Cell Sci **126:**1099–1108. http://dx.doi.org/10.1242/jcs.110932.
38. **Yanagi Y, Takeda M, Ohno S, Hashiguchi T.** 2009. Measles virus receptors. Curr Top Microbiol Immunol **329:**13–30.
39. **Plow EF, Haas TA, Zhang L, Loftus J, Smith JW.** 2000. Ligand binding to integrins. J Biol Chem **275:**21785–21788. http://dx.doi.org/10.1074/jbc.R000003200.
40. **Lepiniec L, Dalgarno L, Huong VT, Monath TP, Digoutte JP, Deubel V.** 1994. Geographic distribution and evolution of yellow fever viruses based on direct sequencing of genomic cDNA fragments. J Gen Virol **75:**417–423. http://dx.doi.org/10.1099/0022-1317-75-2-417.
41. **Barba-Spaeth G, Longman RS, Albert ML, Rice CM.** 2005. Live attenuated yellow fever 17D infects human DCs and allows for presentation of endogenous and recombinant T cell epitopes. J Exp Med **202:**1179–1184. http://dx.doi.org/10.1084/jem.20051352.
42. **van der Most RG, Corver J, Strauss JH.** 1999. Mutagenesis of the RGD motif in the yellow fever virus 17D envelope protein. Virology **265:**83–95. http://dx.doi.org/10.1006/viro.1999.0026.
43. **Germi R, Crance JM, Garin D, Guimet J, Lortat-Jacob H, Ruigrok RW, Zarski JP, Drouet E.** 2002. Heparan sulfate-mediated binding of infectious dengue virus type 2 and yellow fever virus. Virology **292:**162–168. http://dx.doi.org/10.1006/viro.2001.1232.
44. **Nickells J, Cannella M, Droll DA, Liang Y, Wold WS, Chambers TJ.** 2008. Neuroadapted yellow fever virus strain 17D: a charged locus in domain III of the E protein governs heparin binding activity and neuroinvasiveness in the SCID mouse model. J Virol **82:**12510–12519. http://dx.doi.org/10.1128/JVI.00458-08.
45. **Lee E, Hall RA, Lobigs M.** 2004. Common E protein determinants for attenuation of glycosaminoglycan-binding variants of Japanese encephalitis and West Nile viruses. J Virol **78:**8271–8280. http://dx.doi.org/10.1128/JVI.78.15.8271-8280.2004.
46. **Lee E, Lobigs M.** 2002. Mechanism of virulence attenuation of glycosaminoglycan-binding variants of Japanese encephalitis virus and Murray Valley encephalitis virus. J Virol **76:**4901–4911. http://dx.doi.org/10.1128/JVI.76.10.4901-4911.2002.
47. **Lee E, Lobigs M.** 2000. Substitutions at the putative receptor-binding site of an encephalitic flavivirus alter virulence and host cell tropism and reveal a role for glycosaminoglycans in entry. J Virol **74:**8867–8875. http://dx.doi.org/10.1128/JVI.74.19.8867-8875.2000.

48. **Lee E, Wright PJ, Davidson A, Lobigs M.** 2006. Virulence attenuation of dengue virus due to augmented glycosaminoglycan-binding affinity and restriction in extraneural dissemination. J Gen Virol **87:**2791–2801. http://dx.doi.org/10.1099/vir.0.82164-0.
49. **Mandl CW, Kroschewski H, Allison SL, Kofler R, Holzmann H, Meixner T, Heinz FX.** 2001. Adaptation of tick-borne encephalitis virus to BHK-21 cells results in the formation of multiple heparan sulfate binding sites in the envelope protein and attenuation in vivo. J Virol **75:**5627–5637. http://dx.doi.org/10.1128/JVI.75.12.5627-5637.2001.
50. **Bernard KA, Klimstra WB, Johnston RE.** 2000. Mutations in the E2 glycoprotein of Venezuelan equine encephalitis virus confer heparan sulfate interaction, low morbidity, and rapid clearance from blood of mice. Virology **276:**93–103. http://dx.doi.org/10.1006/viro.2000.0546.
51. **Byrnes AP, Griffin DE.** 1998. Binding of Sindbis virus to cell surface heparan sulfate. J Virol **72:**7349–7356.
52. **Sa-Carvalho D, Rieder E, Baxt B, Rodarte R, Tanuri A, Mason PW.** 1997. Tissue culture adaptation of foot-and-mouth disease virus selects viruses that bind to heparin and are attenuated in cattle. J Virol **71:**5115–5123.
53. **Payne CK, Jones SA, Chen C, Zhuang X.** 2007. Internalization and trafficking of cell surface proteoglycans and proteoglycan-binding ligands. Traffic **8:**389–401. http://dx.doi.org/10.1111/j.1600-0854.2007.00540.x.
54. **Bruni D, Chazal M, Sinigaglia L, Chauveau L, Schwartz O, Desprès P, Jouvenet N.** 2015. Viral entry route determines how human plasmacytoid dendritic cells produce type I interferons. Sci Signal **8:**ra25. http://dx.doi.org/10.1126/scisignal.aaa1552.
55. **Mandl JN, Akondy R, Lawson B, Kozyr N, Staprans SI, Ahmed R, Feinberg MB.** 2011. Distinctive TLR7 signaling, type I IFN production, and attenuated innate and adaptive immune responses to yellow fever virus in a primate reservoir host. J Immunol **186:**6406–6416. http://dx.doi.org/10.4049/jimmunol.1001191.
56. **Ye J, Zhu B, Fu ZF, Chen H, Cao S.** 2013. Immune evasion strategies of flaviviruses. Vaccine **31:**461–471. http://dx.doi.org/10.1016/j.vaccine.2012.11.015.
57. **Beck A, Tesh RB, Wood TG, Widen SG, Ryman KD, Barrett AD.** 2014. Comparison of the live attenuated yellow fever vaccine 17D-204 strain to its virulent parental strain Asibi by deep sequencing. J Infect Dis **209:**334–344. http://dx.doi.org/10.1093/infdis/jit546.
58. **Vignuzzi M, Stone JK, Arnold JJ, Cameron CE, Andino R.** 2006. Quasispecies diversity determines pathogenesis through cooperative interactions in a viral population. Nature **439:**344–348. http://dx.doi.org/10.1038/nature04388.
59. **Lozach PY, Amara A, Bartosch B, Virelizier JL, Arenzana-Seisdedos F, Cosset FL, Altmeyer R.** 2004. C-type lectins L-SIGN and DC-SIGN capture and transmit infectious hepatitis C virus pseudotype particles. J Biol Chem **279:**32035–32045.
60. **Rice CM, Grakoui A, Galler R, Chambers TJ.** 1989. Transcription of infectious yellow fever RNA from full-length cDNA templates produced by in vitro ligation. New Biol **1:**285–296.
61. **Pierson TC, Diamond MS, Ahmed AA, Valentine LE, Davis CW, Samuel MA, Hanna SL, Puffer BA, Doms RW.** 2005. An infectious West Nile virus that expresses a GFP reporter gene. Virology **334:**28–40. http://dx.doi.org/10.1016/j.virol.2005.01.021.
62. **Hayer A, Stoeber M, Bissig C, Helenius A.** 2010. Biogenesis of caveolae: stepwise assembly of large caveolin and cavin complexes. Traffic **11:**361–382. http://dx.doi.org/10.1111/j.1600-0854.2009.01023.x.
63. **Meertens L, Bertaux C, Dragic T.** 2006. Hepatitis C virus entry requires a critical postinternalization step and delivery to early endosomes via clathrin-coated vesicles. J Virol **80:**11571–11578. http://dx.doi.org/10.1128/JVI.01717-06.
64. **Subtil A, Hémar A, Dautry-Varsat A.** 1994. Rapid endocytosis of interleukin 2 receptors when clathrin-coated pit endocytosis is inhibited. J Cell Sci **107:**3461–3468. http://dx.doi.org/10.1016/0248-4900(96)81369-4.
65. **Oliphant T, Engle M, Nybakken GE, Doane C, Johnson S, Huang L, Gorlatov S, Mehlhop E, Marri A, Chung KM, Ebel GD, Kramer LD, Fremont DH, Diamond MS.** 2005. Development of a humanized monoclonal antibody with therapeutic potential against West Nile virus. Nat Med **11:**522–530. http://dx.doi.org/10.1038/nm1240.
66. **Brault JB, Kudelko M, Vidalain PO, Tangy F, Desprès P, Pardigon N.** 2011. The interaction of flavivirus M protein with light chain Tctex-1 of human dynein plays a role in late stages of virus replication. Virology **417:**369–378. http://dx.doi.org/10.1016/j.virol.2011.06.022.
67. **Snijder B, Sacher R, Rämö P, Liberali P, Mench K, Wolfrum N, Burleigh L, Scott CC, Verheije MH, Mercer J, Moese S, Heger T, Theusner K, Jurgeit A, Lamparter D, Balistreri G, Schelhaas M, De Haan CA, Marjomäki V, Hyypiä T, Rottier PJ, Sodeik B, Marsh M, Gruenberg J, Amara A, Greber U, Helenius A, Pelkmans L.** 2012. Single-cell analysis of population context advances RNAi screening at multiple levels. Mol Syst Biol **8:**579. http://dx.doi.org/10.1038/msb.2012.9.
68. **Lozach PY, Burleigh L, Staropoli I, Navarro-Sanchez E, Harriague J, Virelizier JL, Rey FA, Desprès P, Arenzana-Seisdedos F, Amara A.** 2005. Dendritic cell-specific intercellular adhesion molecule 3-grabbing nonintegrin (DC-SIGN)-mediated enhancement of dengue virus infection is independent of DC-SIGN internalization signals. J Biol Chem **280:**23698–23708. http://dx.doi.org/10.1074/jbc.M504337200.
69. **Meertens L, Carnec X, Lecoin MP, Ramdasi R, Guivel-Benhassine F, Lew E, Lemke G, Schwartz O, Amara A.** 2012. The TIM and TAM families of phosphatidylserine receptors mediate dengue virus entry. Cell Host Microbe **12:**544–557. http://dx.doi.org/10.1016/j.chom.2012.08.009.
70. **Grassart A, Meas-Yedid V, Dufour A, Olivo-Marin JC, Dautry-Varsat A, Sauvonnet N.** 2010. Pak1 phosphorylation enhances cortactin-N-WASP interaction in clathrin-caveolin-independent endocytosis. Traffic **11:**1079–1091. http://dx.doi.org/10.1111/j.1600-0854.2010.01075.x.
71. **Basquin C, Malardé V, Mellor P, Anderson DH, Meas-Yedid V, Olivo-Marin JC, Dautry-Varsat A, Sauvonnet N.** 2013. The signalling factor PI 3-kinase is a specific regulator of the clathrin-independent dynamin-dependent endocytosis of IL-2 receptors. J Cell Sci **126:**1099–1108. http://dx.doi.org/10.1242/jcs.110932.